



上海交通大学
SHANGHAI JIAO TONG UNIVERSITY



[O16-2]

Accelerated development of thermally stable Nd-Fe-B magnets with light rare-earth elements and their synergetic effects to temperature stability with Co

Xinyi Ji¹, Lanting Zhang¹, Hong Zhu², Zhaozhe Zhong³, Jian Liu³,
Zhanji Dong⁴, Zhongjie Peng⁴, Kaihong Ding⁴

1. School of Materials Science and Engineering, Shanghai Jiao Tong University, 800 Dongchuan Road, Shanghai 200240, China
2. University of Michigan-Shanghai Jiao Tong University Joint Institute, Shanghai Jiao Tong University, 800 Dongchuan Road, Shanghai 200240, China
3. Advanced Engineering Research Division, Toyota Motor Technical Research and Service (Shanghai) Co., Ltd, 6333 North Jiasong Road, Shanghai 201804, China
4. Yantai Dongxing Magnetic Materials Inc., 888 Yongda Street, Yantai 265500, China



Background

HEV/EV



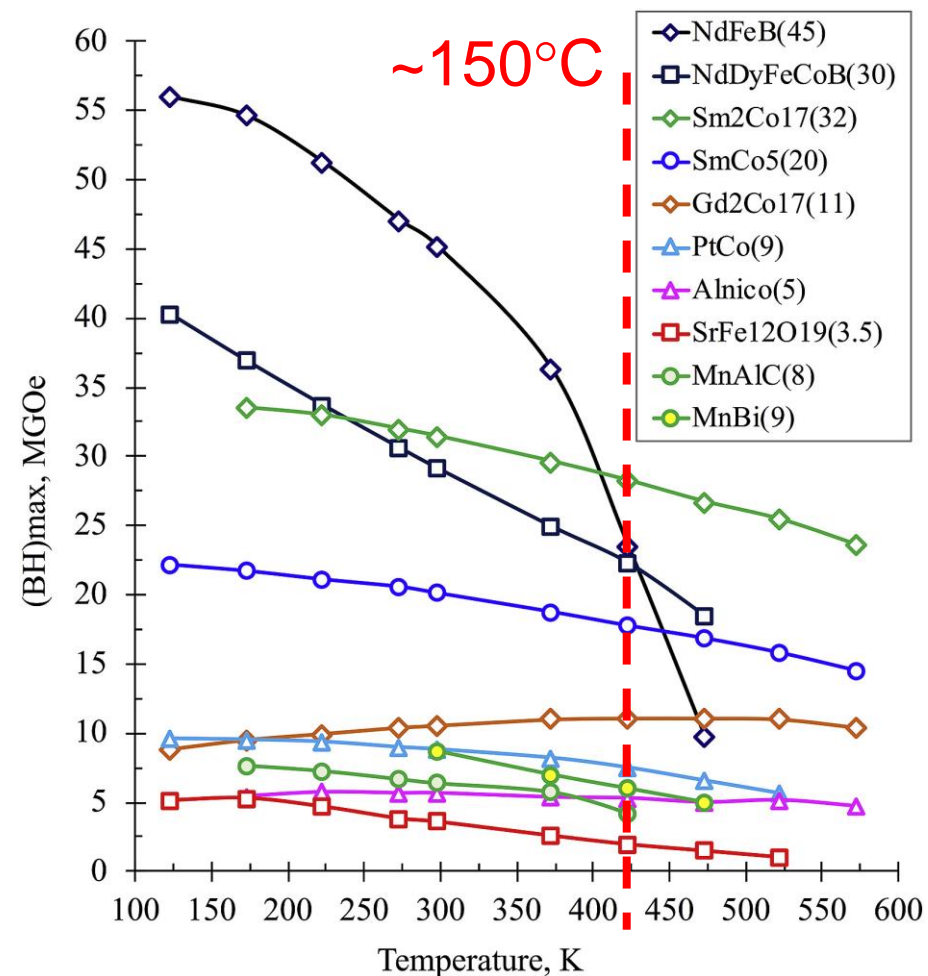
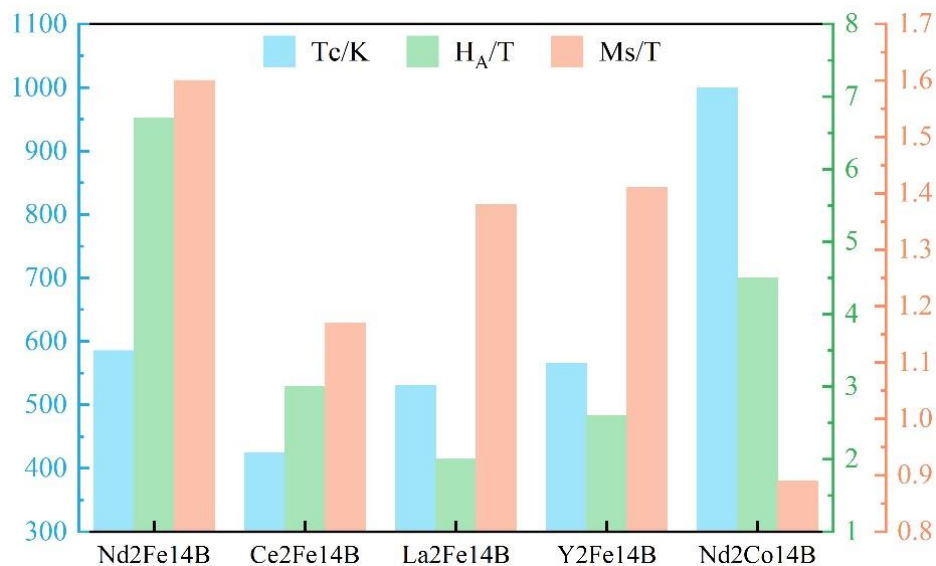
Wind turbine



Robot



Perform/cost is an everlasting topic in engineering.

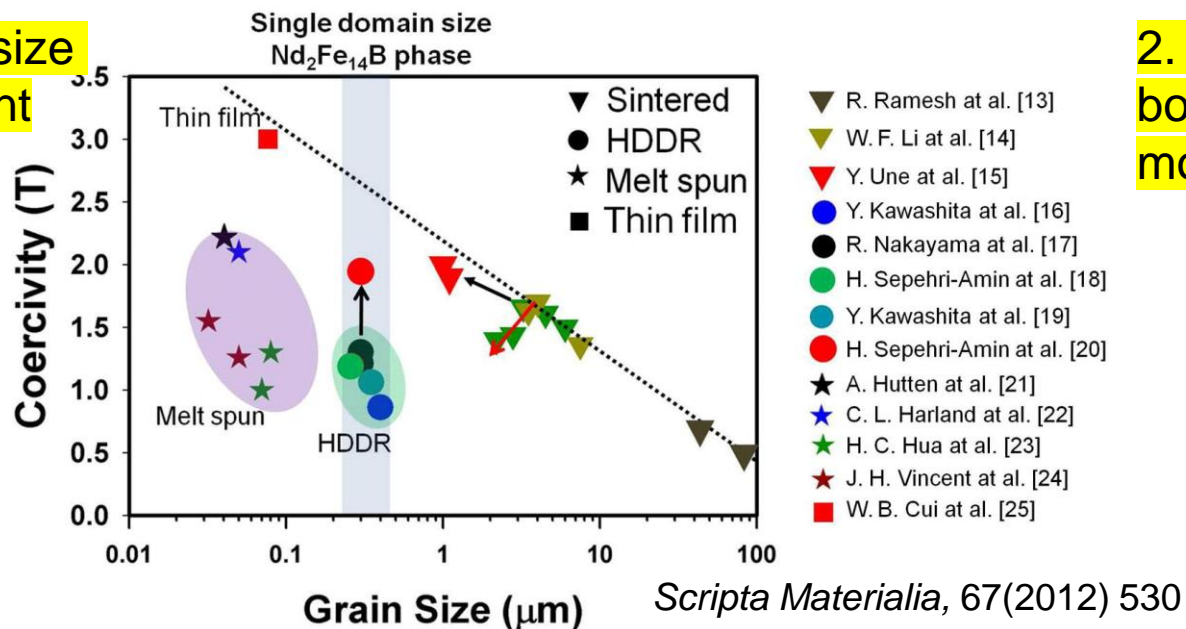


Acta Materialia, 158 (2018) 118-137, <https://doi.org/10.1016/j.actamat.2018.07.049>

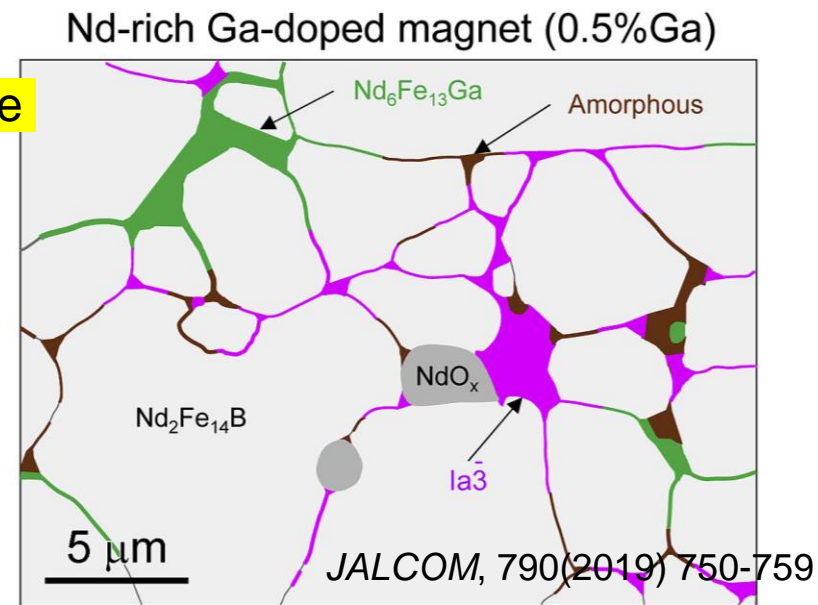


Attempts on Nd-Fe-B-based magnets

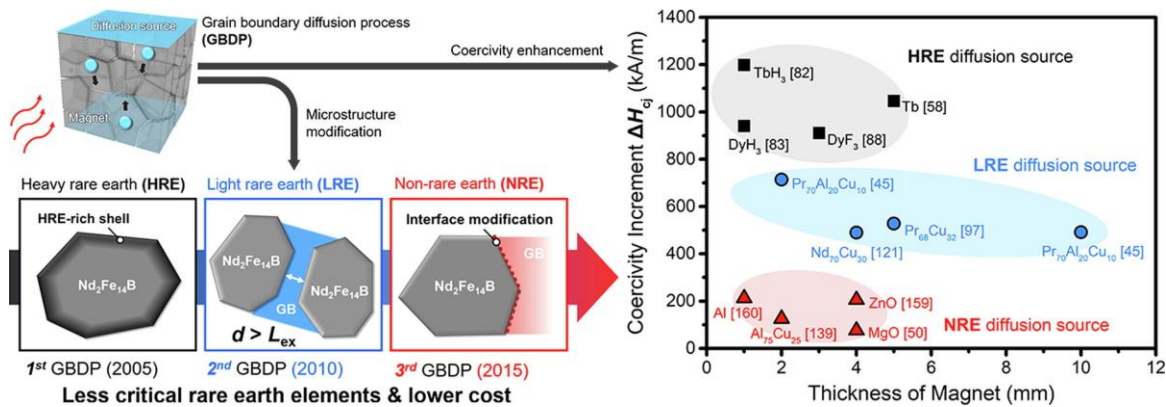
1. Grain size refinement



2. Grain boundary phase modification

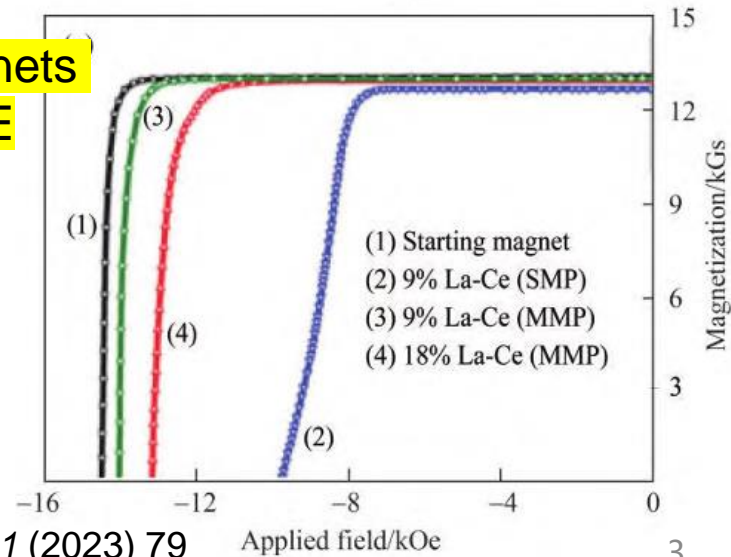


3. Grain boundary diffusion process



Materials & Design 209 (2021) 110004

4. Cost-effective magnets w. high abundance RE



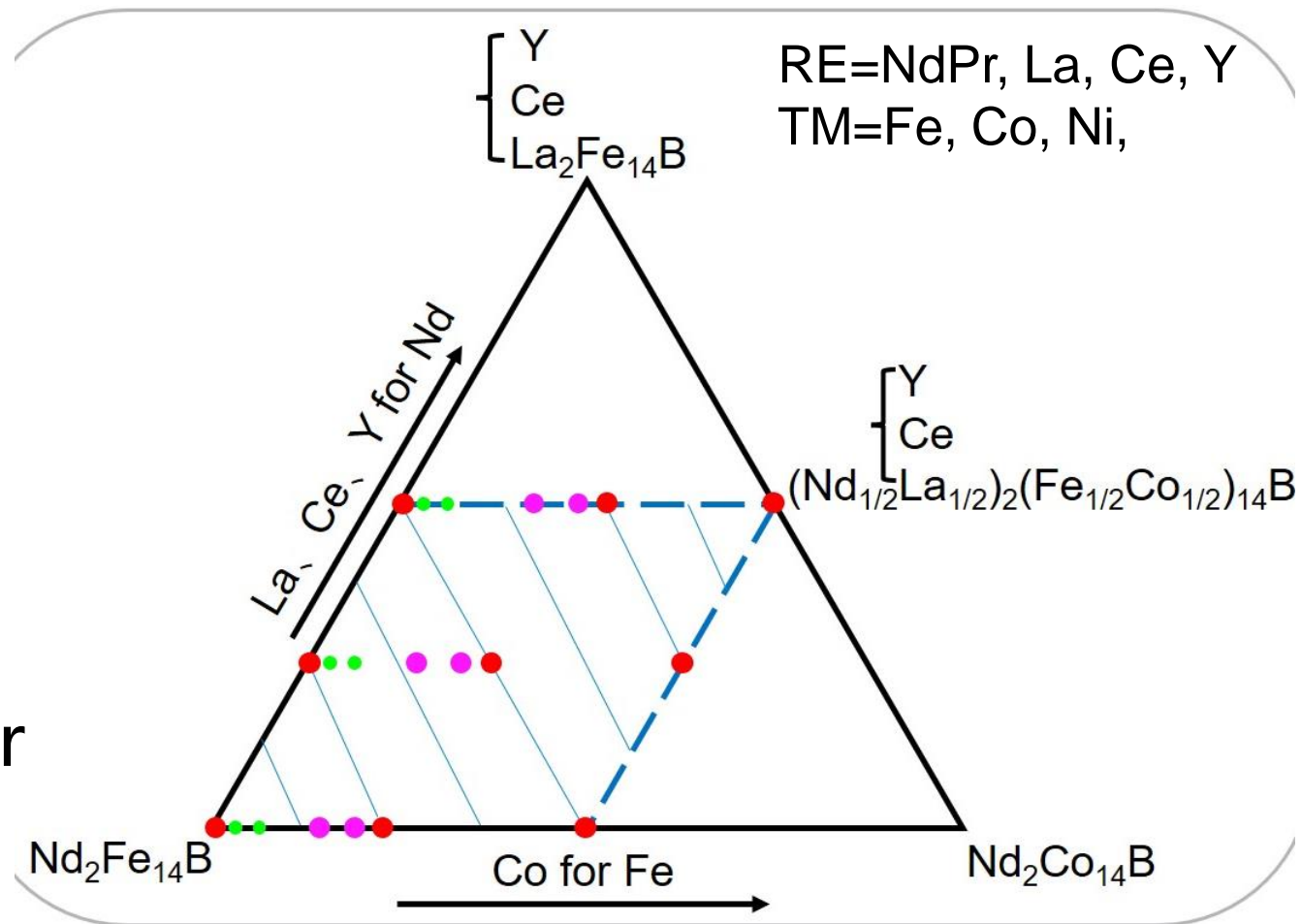
J. Chn Soc. Rare Earths 41 (2023) 79

Applied field/kOe



The purpose of this work

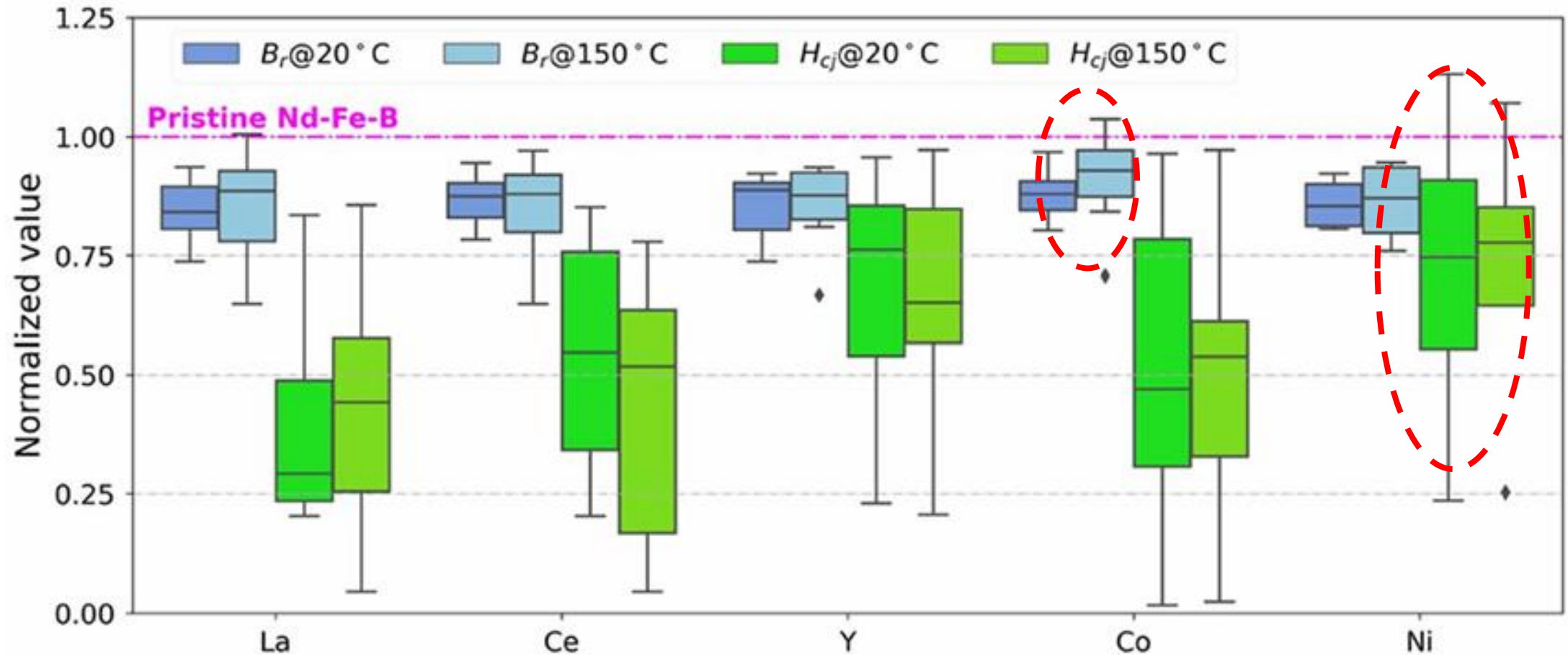
- To explore magnets with exceptional high temperature stability at $\sim 150^\circ\text{C}$ and above.
- Use cost-effective LREs for the performance cost of magnet instead of using HREs, high- T_c elements.
- Development under the near mass-production condition.





Magnetic properties of the 24 starting compos.

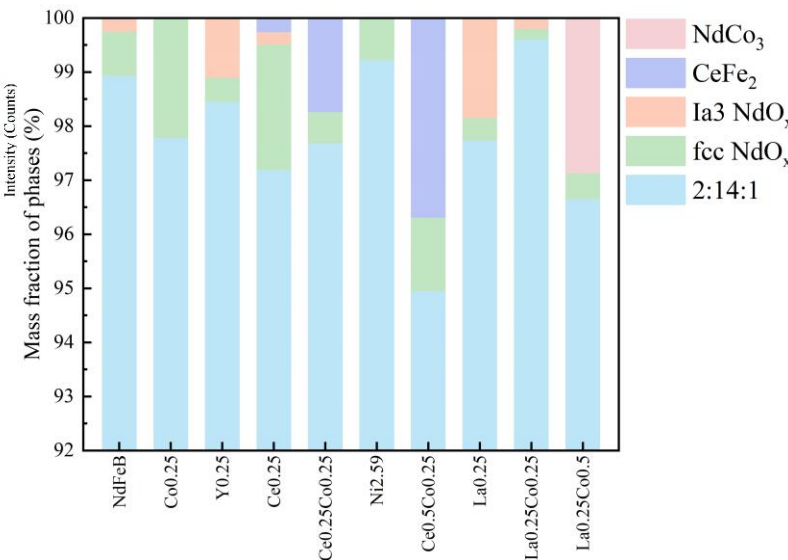
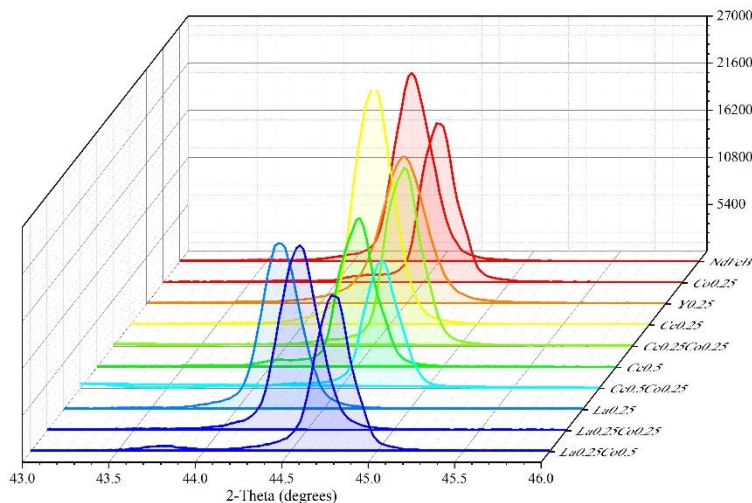
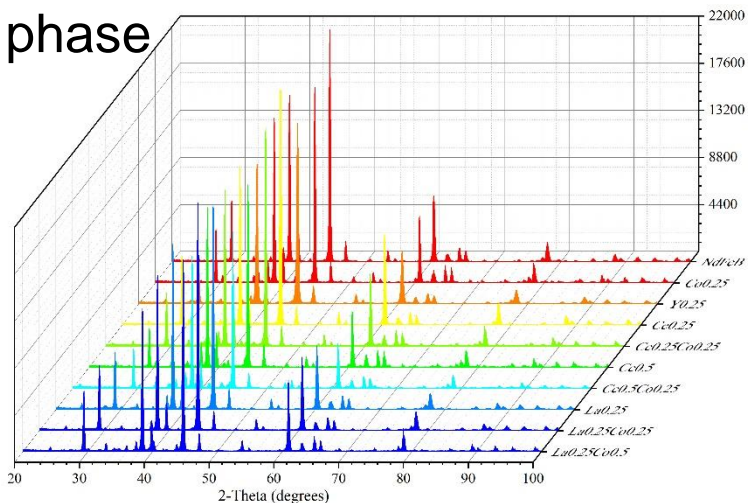
1. For Br@150°C, higher values than that of pristine Nd-Fe-B could be achieved at a high doping level of Co.
2. A decrease in H_{cj} is observed for all the doping species except Ni.



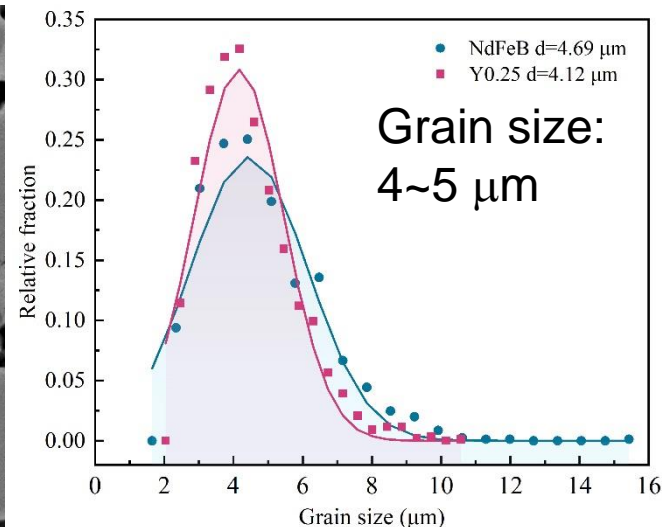
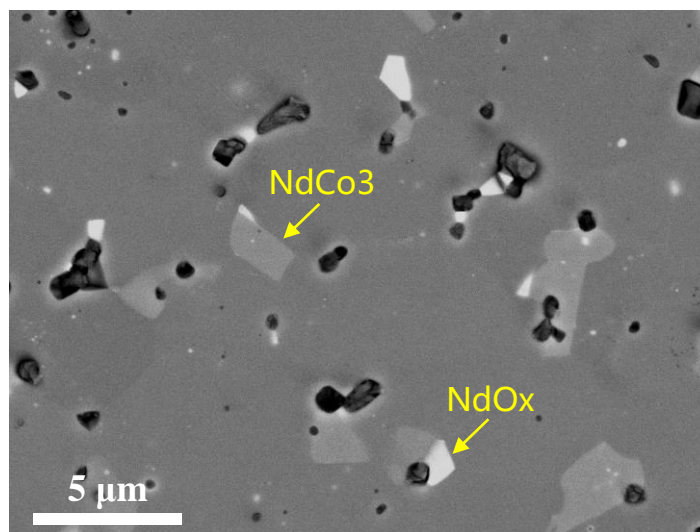
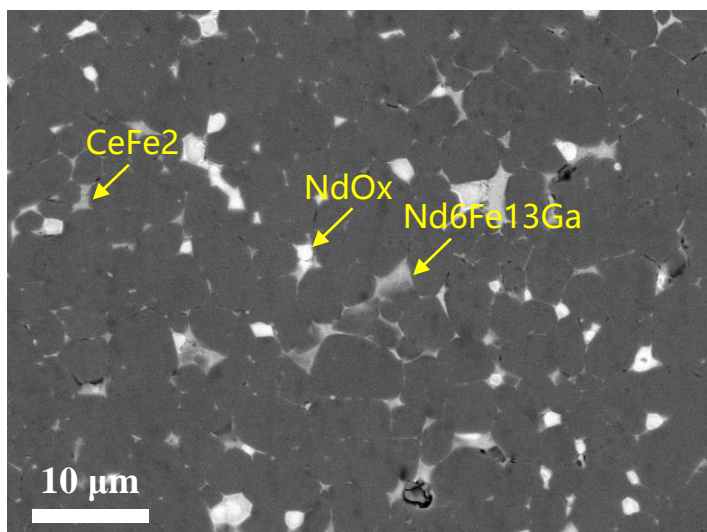


Phase constitution and microstructure of the magnets

2:14:1 phase
>95%



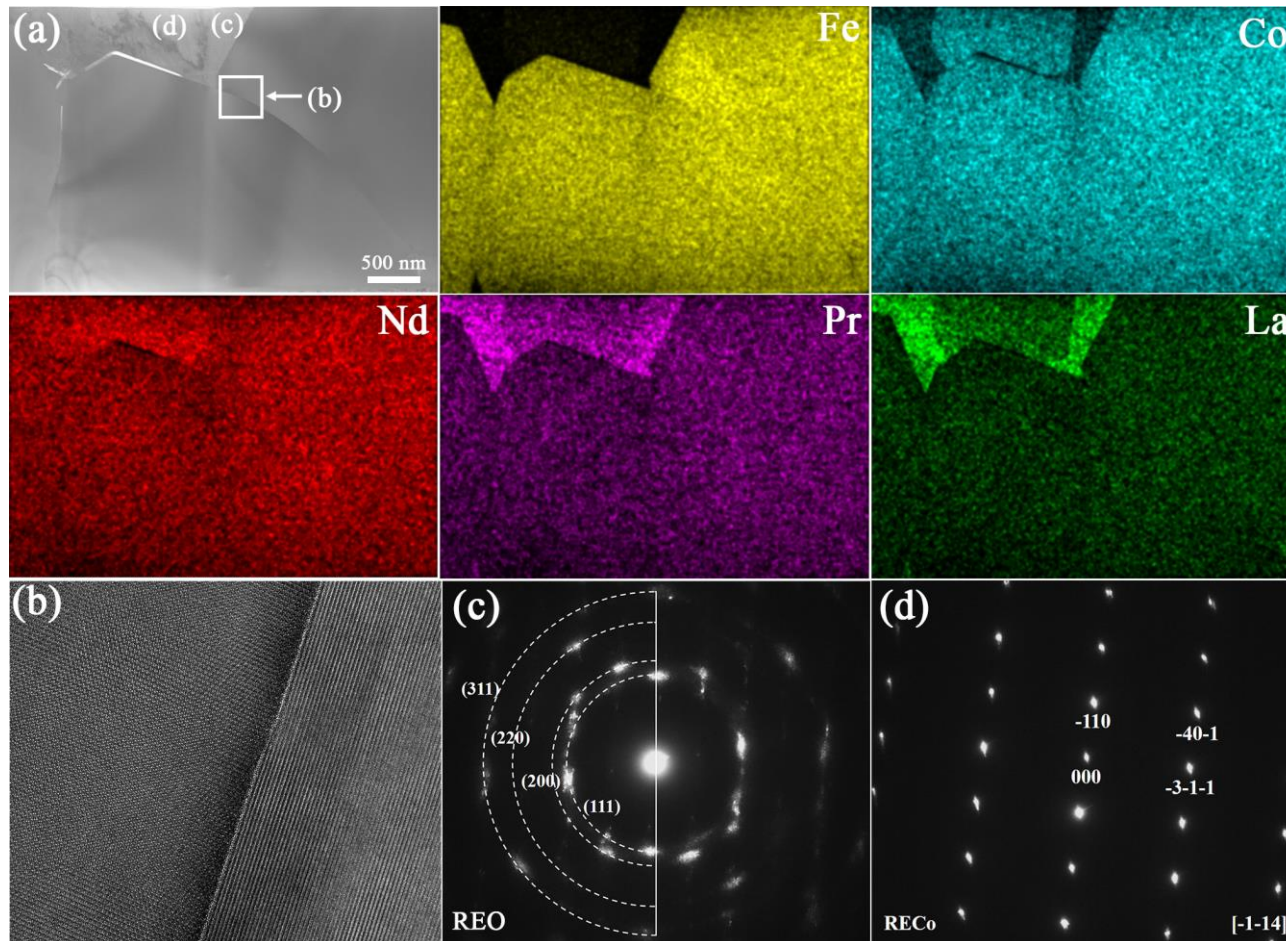
Microstructure



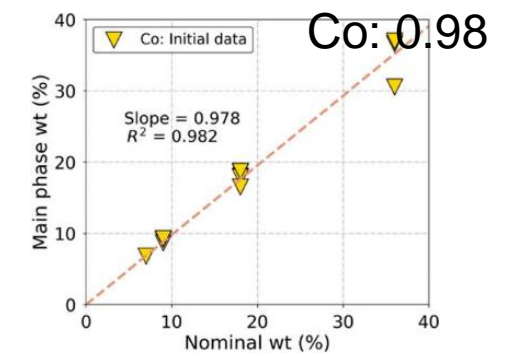
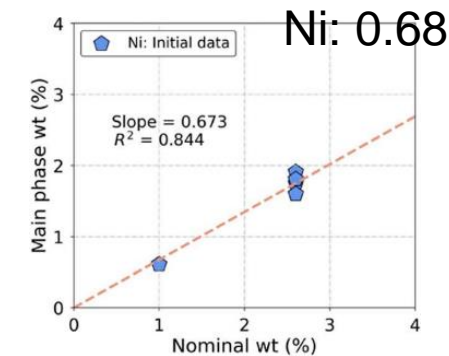
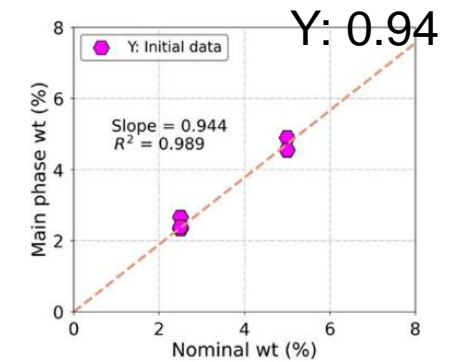
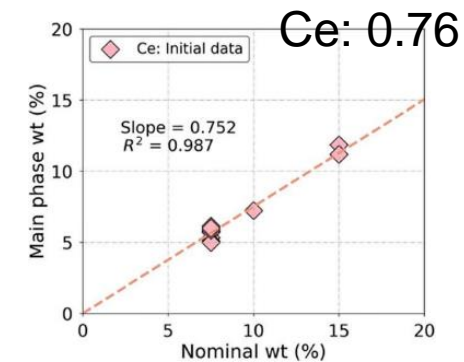
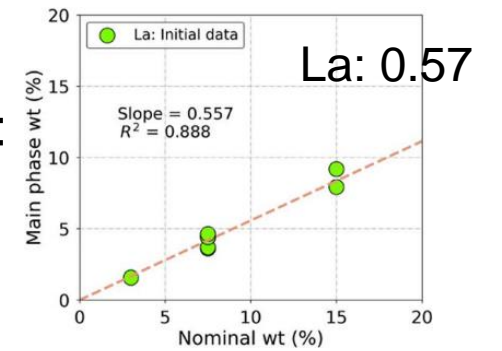


Phase constitution and microstructure of the magnets

Details at GB in a $\text{La}_{0.25}\text{Co}_{0.25}$ magnet

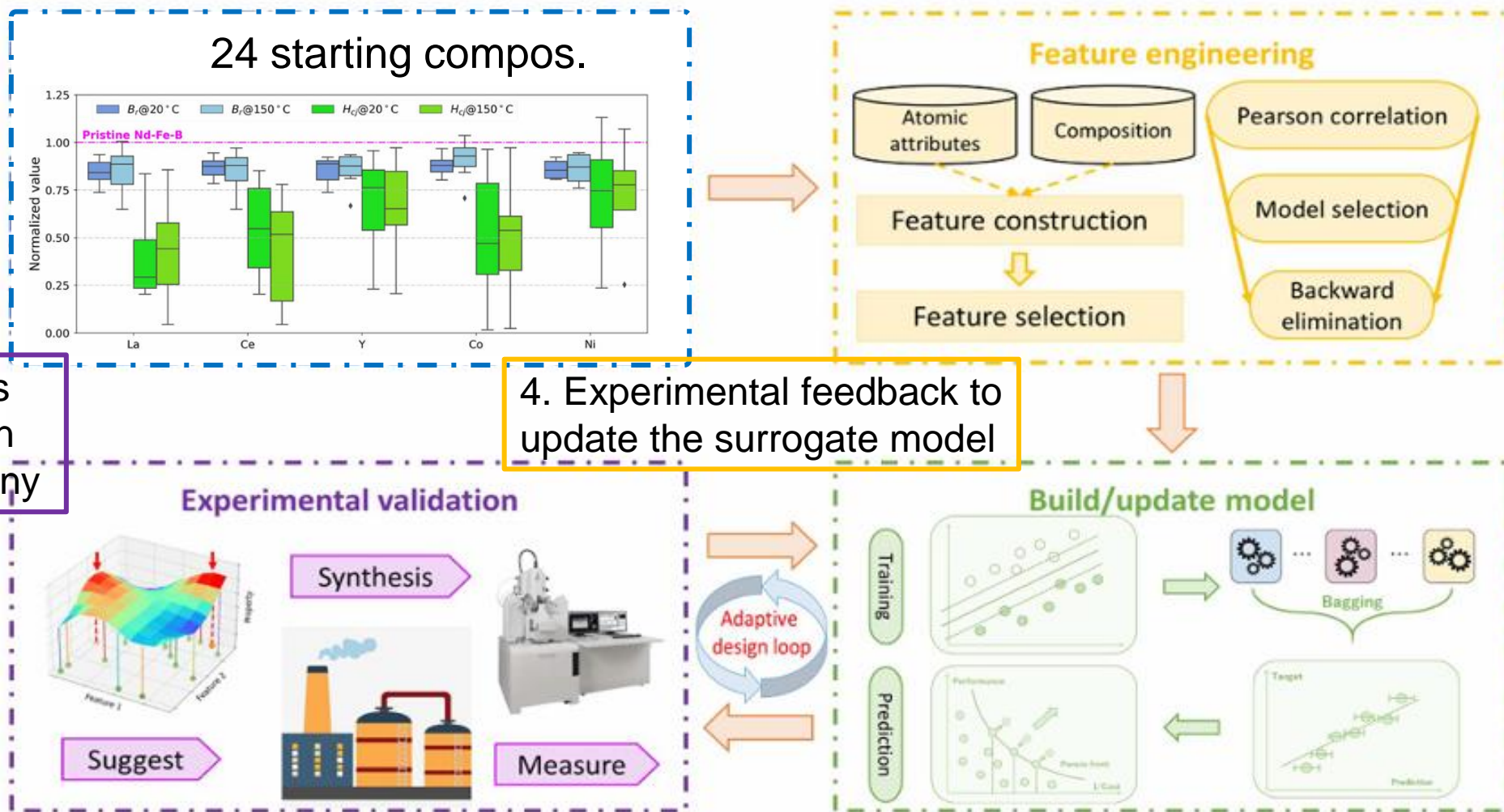


Partitioning behavior:
 $\frac{\text{Main phase wt.}\%}{\text{Nominal wt.}\%}$





The adaptive-learning framework



3. Magnets prepared in the company

4. Experimental feedback to update the surrogate model

2. Bayesian Optimization (BO) to make recommendations to max. optimal candidate



Model construction

1. 16 atomic features

Atomic feature
Atomic number Z_R (Z_T)
Atomic radii r_R (r_T)
Electronegativity χ_R (χ_T)
Atomic mass m_R (m_T)
Valence electron number VEN_R (VEN_T)
Spin angular moment S_{4f} (S_{3d})
Orbital angular moment L_{4f} (L_{3d})
Ionization potential IP_R (IP_T)
Density ρ_R (ρ_T)
Melting point Tm_R (Tm_T)
Boiling point Tb_R (Tb_T)
Enthalpy of fusion Ef_R (Ef_T)
Enthalpy of vaporization Ev_R (Ev_T)
Enthalpy of atomization Ea_R (Ea_T)
Curie Temperature Tc_R (Tc_T)
Saturation magnetization μ_R (μ_T)

2. Feature engineering

Estimator	Selected Features	$B_r@20^\circ\text{C}: \text{CV}$	$B_r@150^\circ\text{C}: \text{CV}$
GP	$[IP_{RT}', 'x_{RT}', 'Ev_R', 'Ef_{RT}']$	0.6	0.83
SVR	$[Tc_T', 'Tc_{RT}', 'IP_{RT}', '\mu_{RT}', 'Ev_R', 'IP_T']$	0.39	0.61
Ridge	$[Tc_{RT}', 'IP_T', 'Ev_R', 'Ea_{RT}']$	0.50	0.89
KNN	$[L4f_R', 'Ea_{RT}', 'IP_T', 'm_R', 'Ef_R']$	0.62	0.83
ANN	$[\mu_T', '\mu_R', '\mu_{RT}', 'r_R', 'm_R', 'IP_T']$	0.57	1.07
DT	$[L4f_R', 'Tm_{RT}', 'Tc_{RT}']$	0.74	0.85

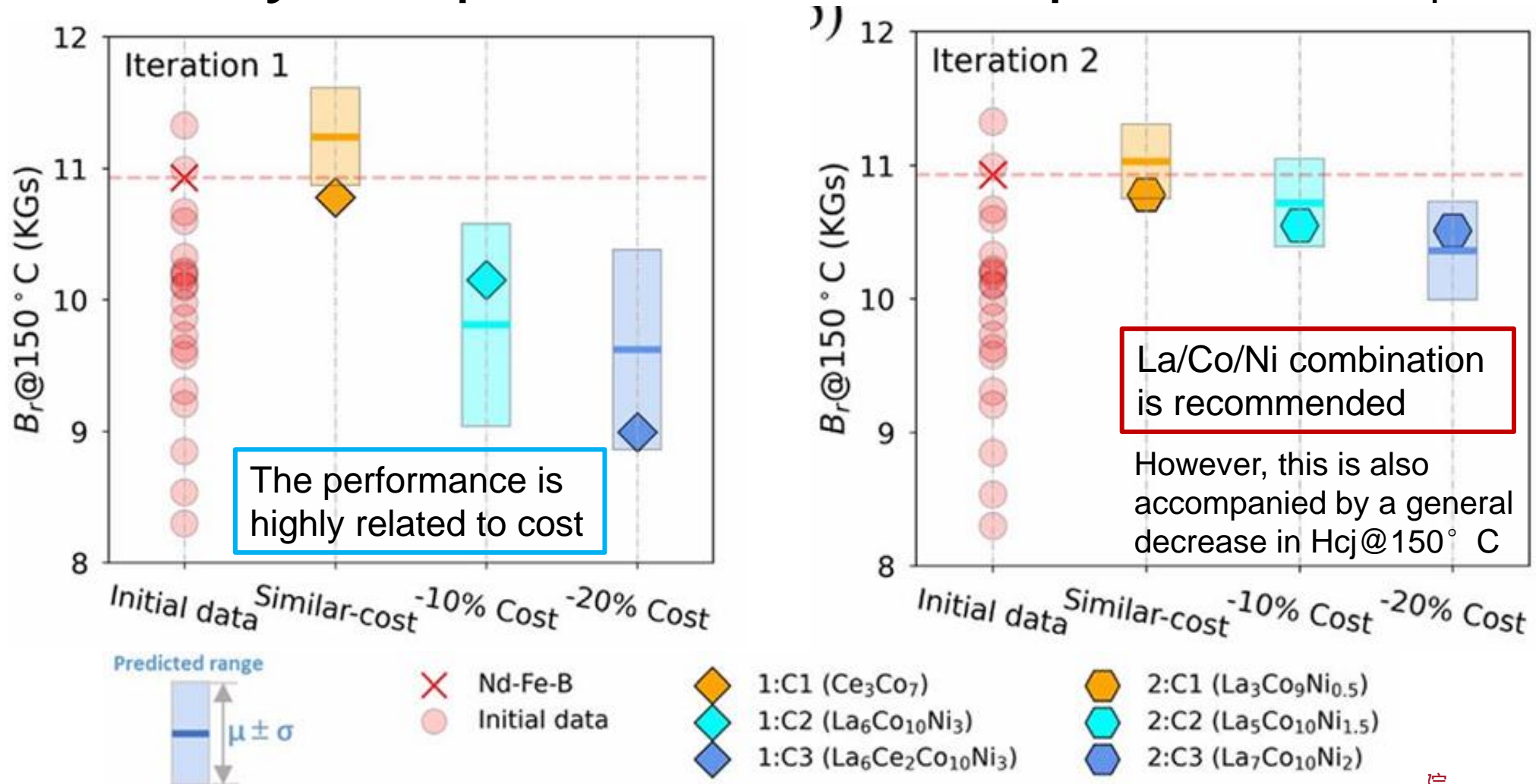
3. Uncertainty estimation: booststrapping

4. Acquisition function: upper confidence bound



Stage 1 optimization: $B_r@150^\circ\text{C}$

- To identify compositions with exceptional HT B_r

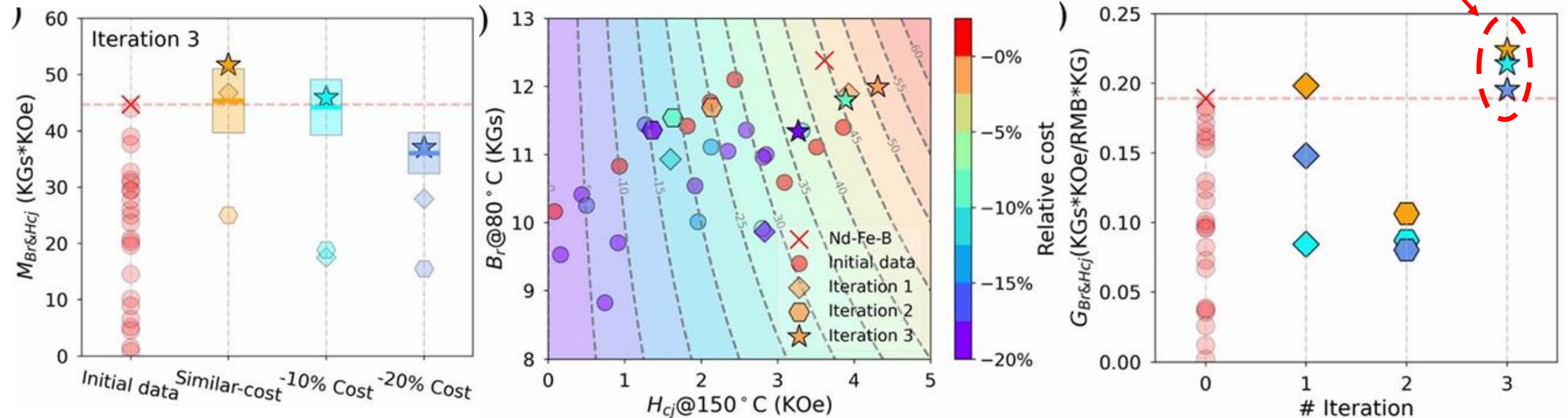




Stage 2 optimization: $B_r@80^\circ\text{C} * H_{cj}@150^\circ\text{C}$

- To improve the overall performance

Improved performance-cost ratio



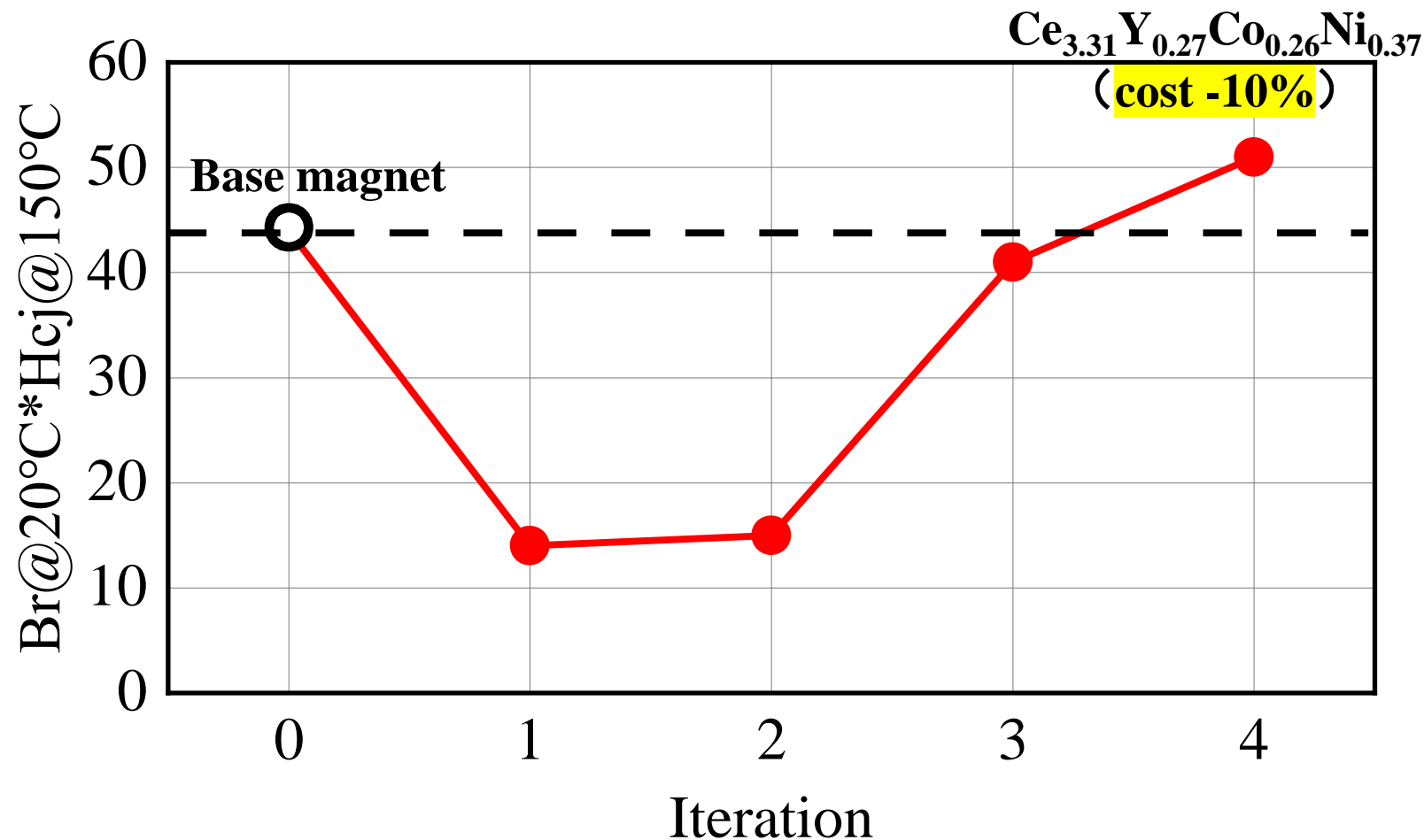
- ★ 3:C1 (Ce_1Co_1)
- ★ 3:C2 ($\text{La}_1\text{Ce}_1\text{Ni}_{0.25}$)
- ★ 3:C3 ($\text{Ce}_5\text{Y}_{0.5}\text{Co}_1$)
- ◇ 2:C1 ($\text{La}_3\text{Co}_9\text{Ni}_{0.5}$)
- ◇ 2:C2 ($\text{La}_5\text{Co}_{10}\text{Ni}_{1.5}$)
- ◇ 2:C3 ($\text{La}_7\text{Co}_{10}\text{Ni}_2$)
- ◇ 1:C1 (Ce_3Co_7)
- ◇ 1:C2 ($\text{La}_6\text{Co}_{10}\text{Ni}_3$)
- ◇ 1:C3 ($\text{La}_6\text{Ce}_2\text{Co}_{10}\text{Ni}_3$)

Performance-cost ratio: $G_{Br\&H_{cj}} = M_{Br\&H_{cj}} / \text{cost}$

The best two candidates showed 18.4% (3: C1) and 13.1% (3: C2) improvement in performance-cost ratio with respect to benchmark Nd-Fe-B



Evolution of properties after iteration

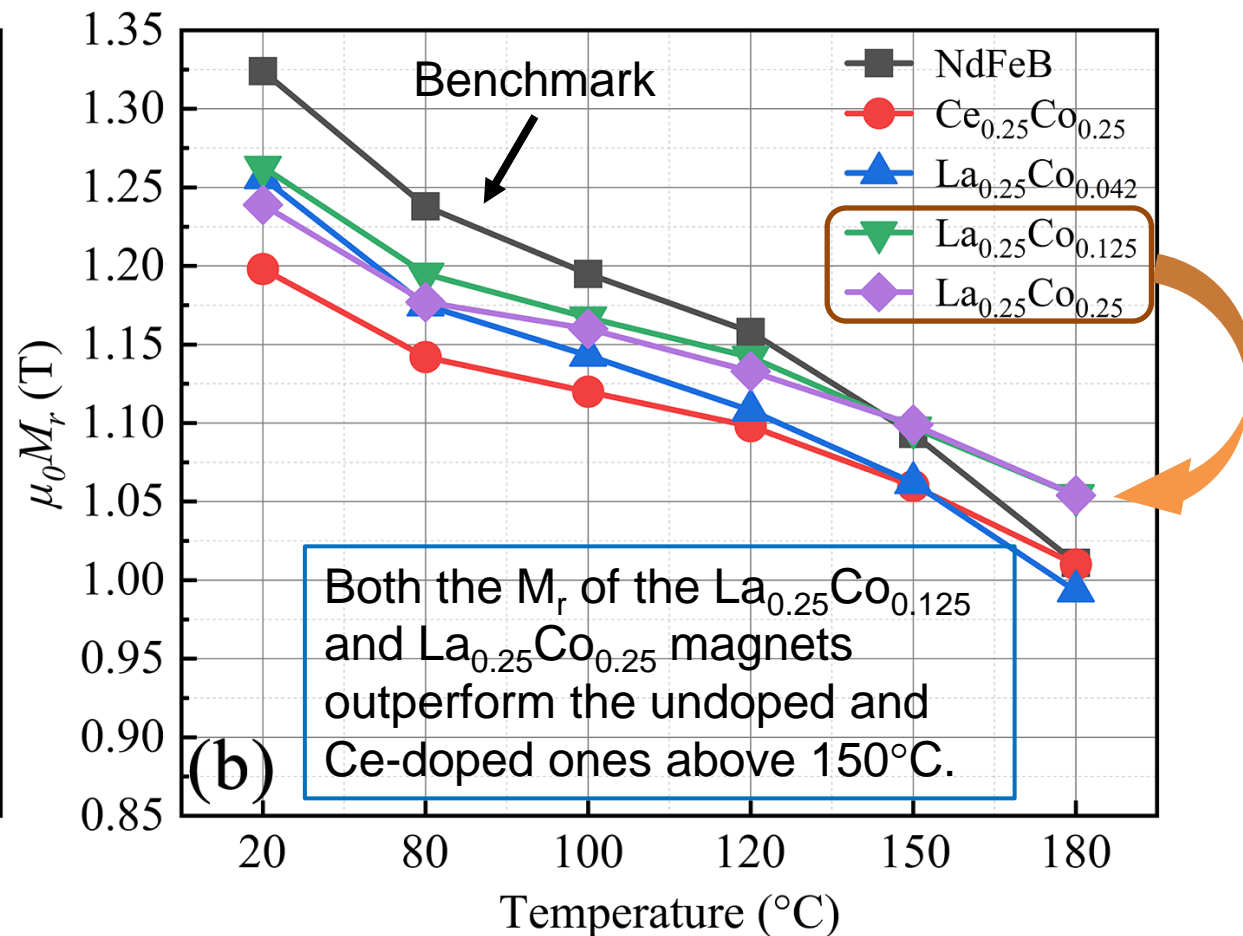
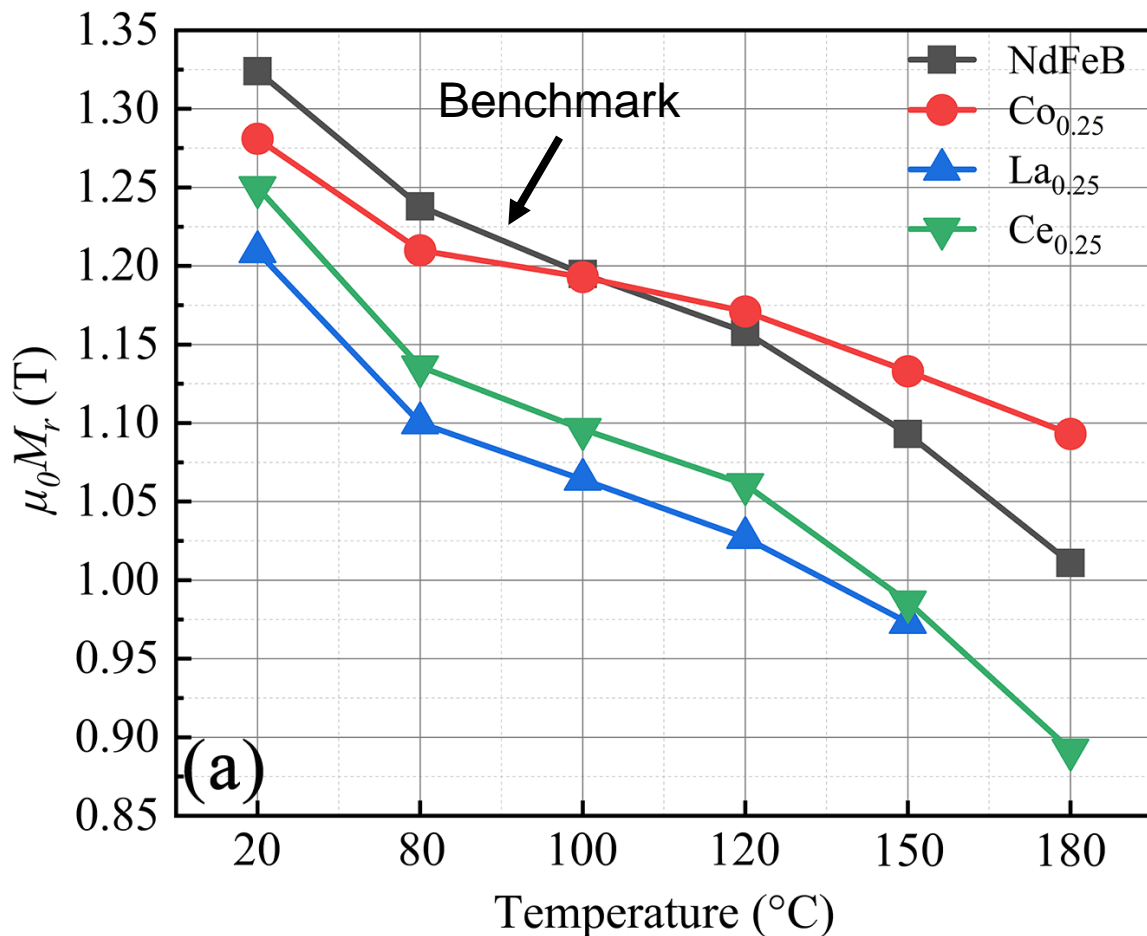
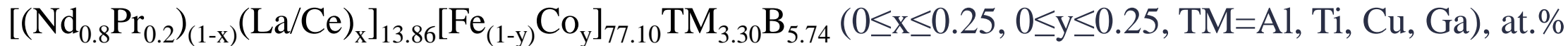


- The La-Co, Ce-Co, La-Co-Ni combinations outperform the other combinations.

- After 4 rounds of iteration, composition with higher performance to the base composition but 10% lower cost was found.



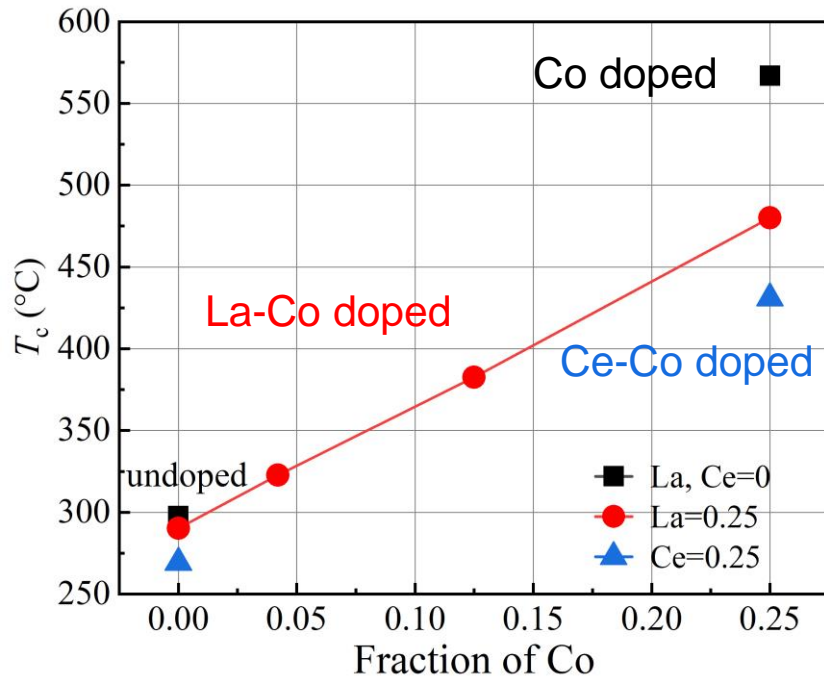
The La-Co pairs w/. higher M_r above 150°C



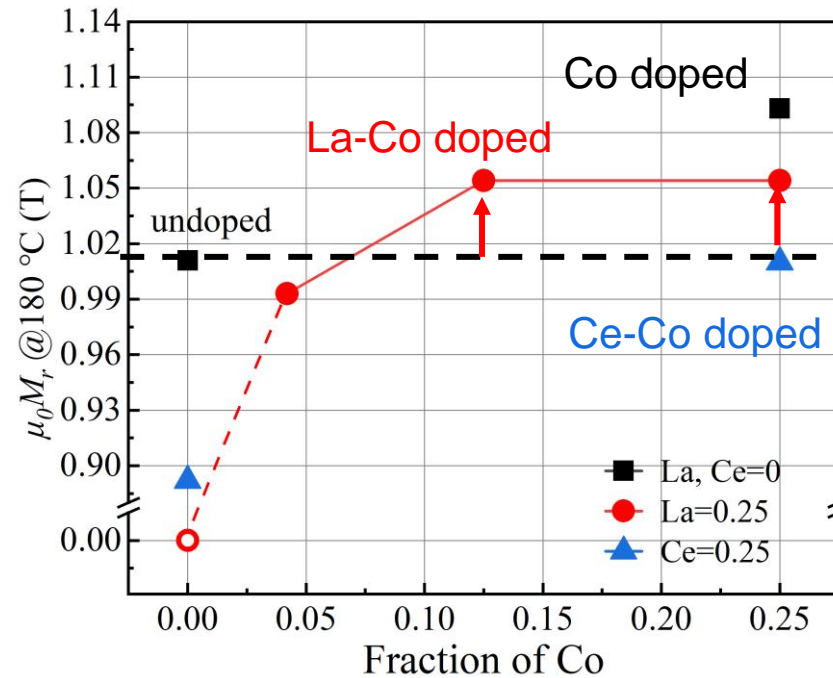


Effect of LRE-Co pair on T stability of M_r

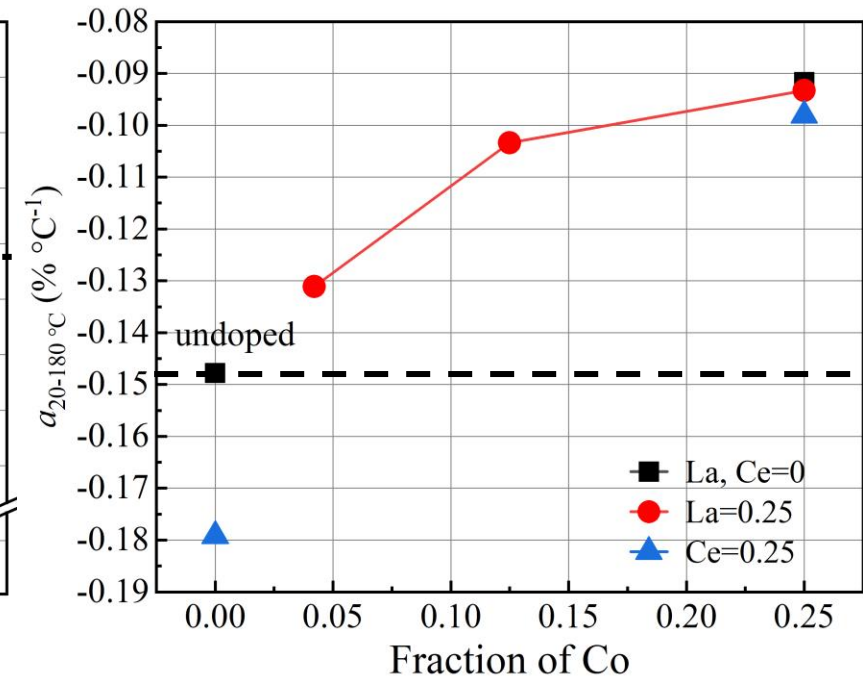
Curie temperature



M_r @180°C



$$\alpha(T) = \frac{\mu_0 M_r(180^\circ\text{C}) - \mu_0 M_r(20^\circ\text{C})}{\mu_0 M_r(20^\circ\text{C}) \times \Delta T}$$



- Without Co, the M_r @180°C of La-doped magnet is inferior to that of Ce-doped one
- For $\text{La}_{0.25}\text{Co}_{0.125}$, higher M_r @180°C despite its lower T_c than $\text{Ce}_{0.25}\text{Co}_{0.25}$
- The $\text{La}_{0.25}\text{Co}_{0.25}$ and $\text{Ce}_{0.25}\text{Co}_{0.25}$ magnets demonstrate almost the same α as that of the $\text{Co}_{0.25}$ even though much lower T_c

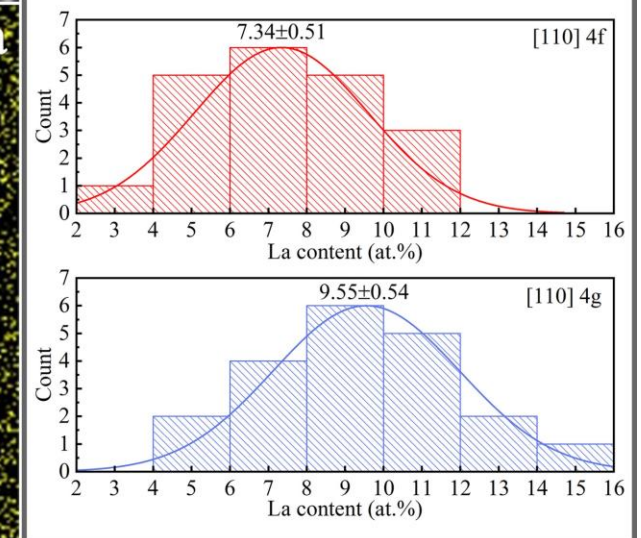
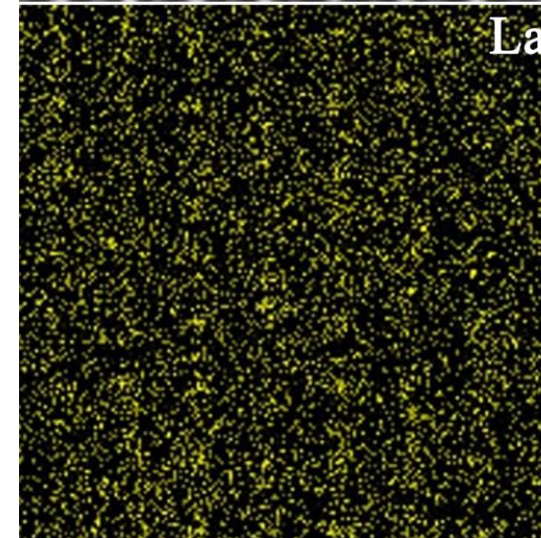
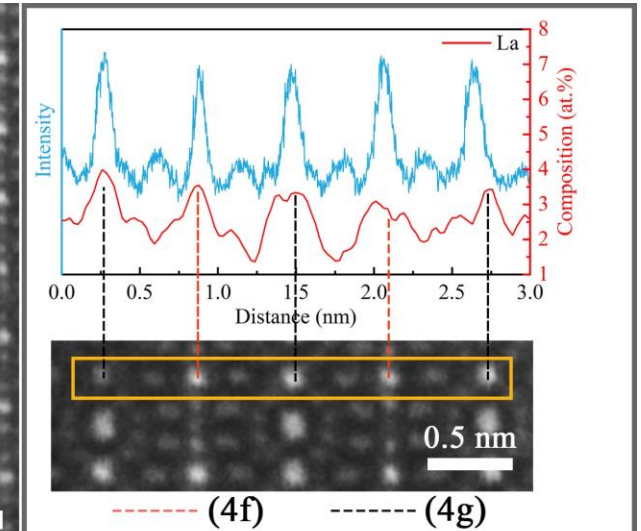
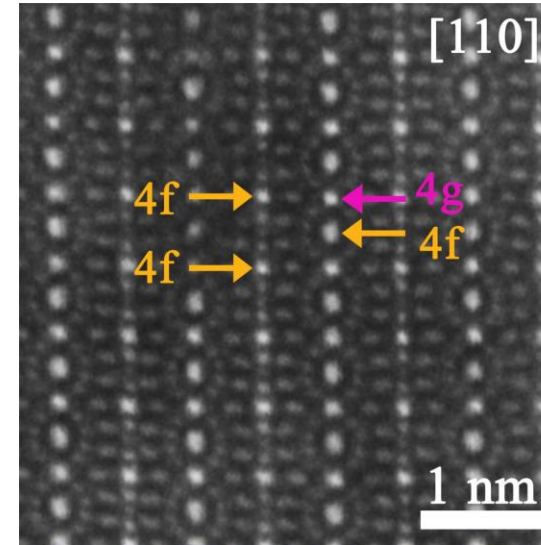
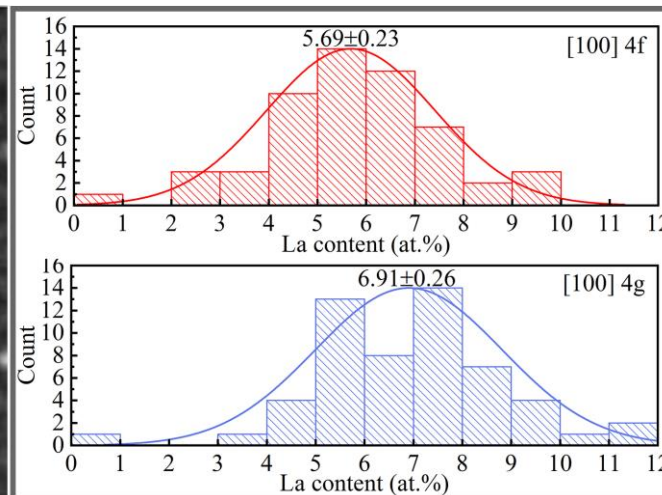
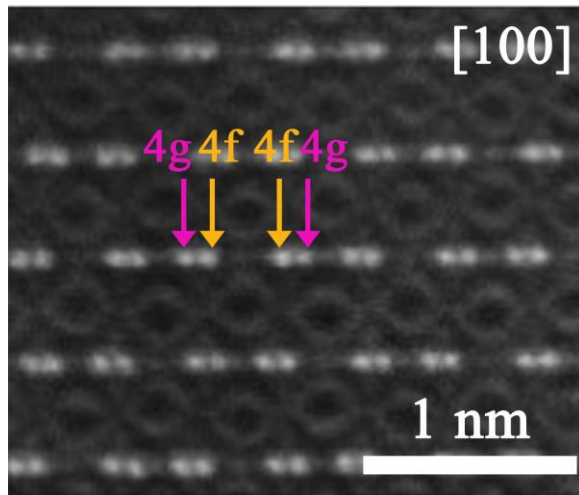


Preferential site occupation of La

- $\text{La}_{0.25}\text{Co}_{0.25}$, La preferentially occupies the 4g-site

La concentration (at.%)

Zone axis	4g-site	4f-site
[110]	9.55 ± 0.54	7.34 ± 0.51
[100]	6.91 ± 0.26	5.69 ± 0.23



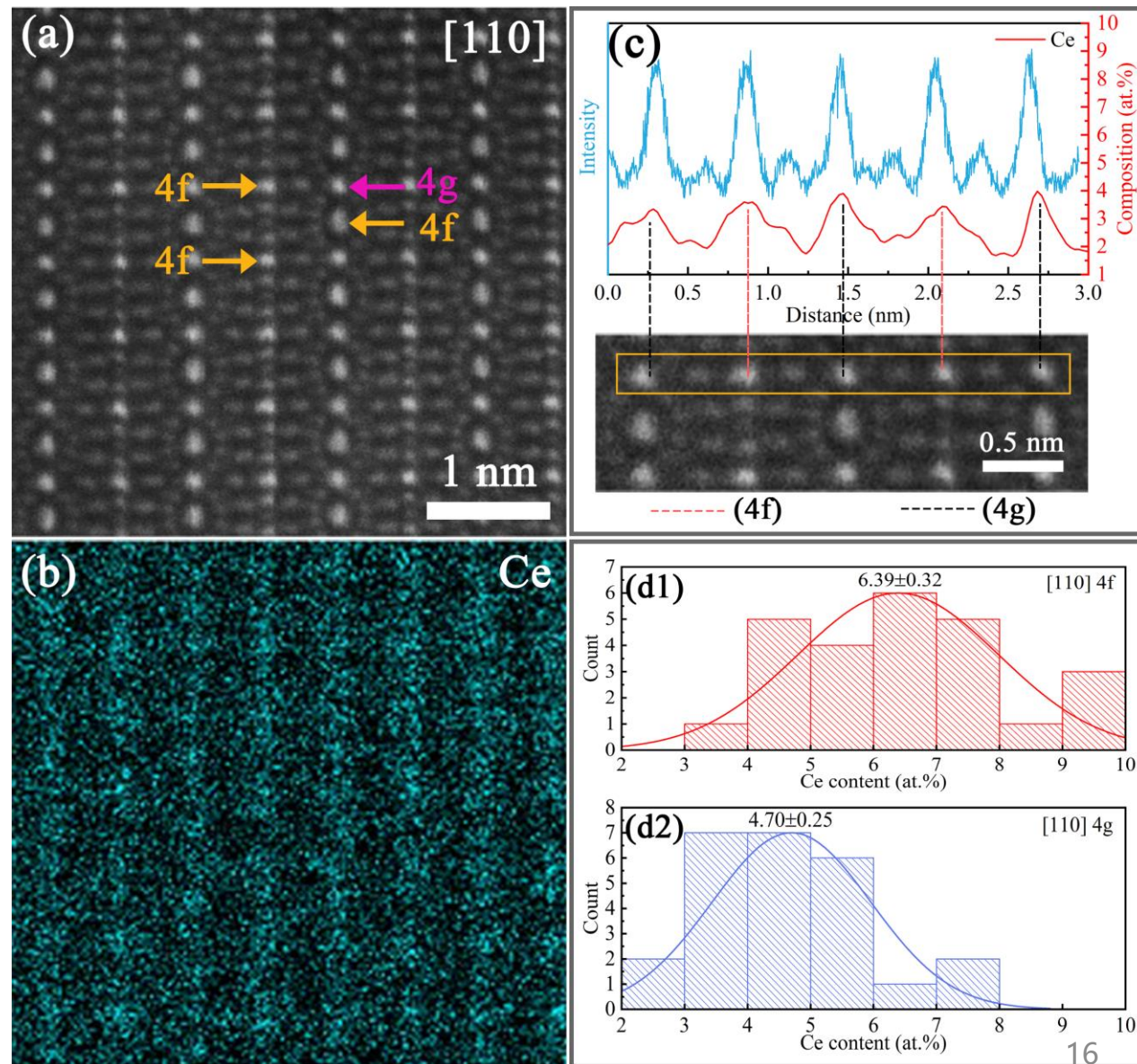


Preferential site occupation of Ce

- $\text{Ce}_{0.25}\text{Co}_{0.25}$
- Ce preferentially occupies the 4f-site

Ce concentration (at.%)

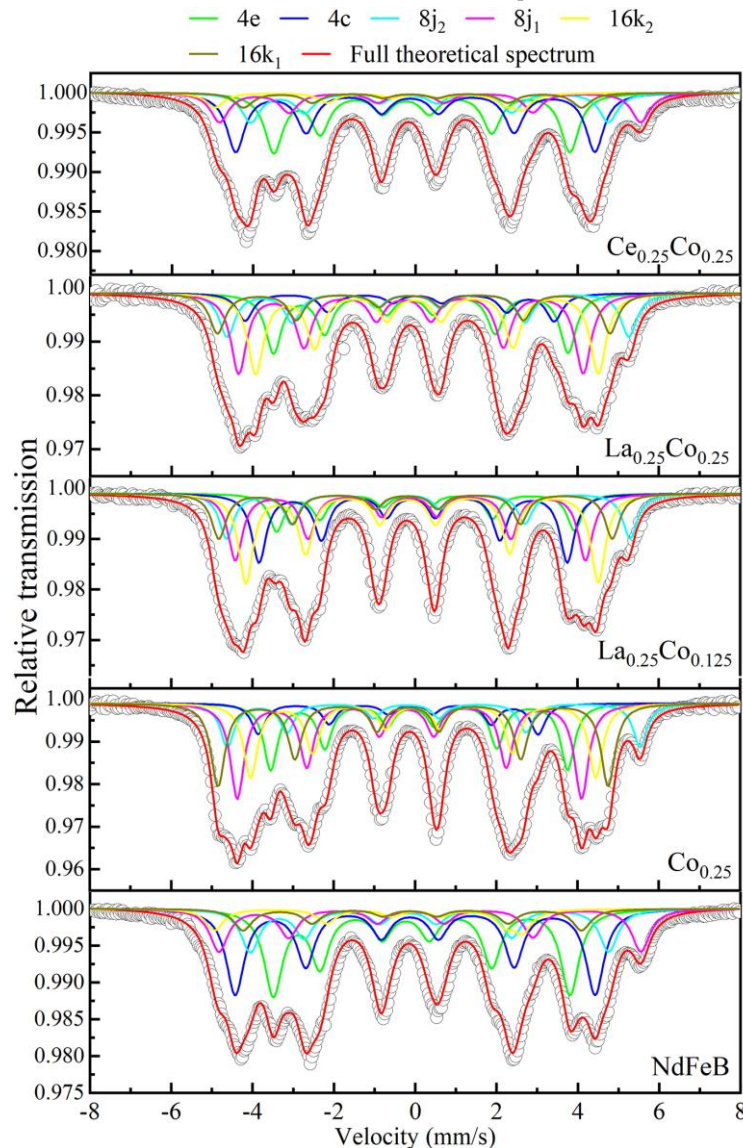
Zone axis	4g-site	4f-site
[110]	4.70 ± 0.25	6.39 ± 0.32





Preferential site occupations of Co

Mössbauer spectra



Refined relative areas ($\pm 1\%$) of the Fe sites in the lattice

Fe site	Undoped	Co _{0.25}	La _{0.25} Co _{0.125}	La _{0.25} Co _{0.25}	Ce _{0.25} Co _{0.25}
16k ₁	28.57	21.09	12.86	12.12	26.42
16k ₂	28.57	18.88	25.28	24.24	20.85
8j ₁	14.29	24.18	18.96	24.15	11.95
8j ₂	14.29	11.11	12.77	13.15	16.20
4c	7.14	7.85	19.5	8.37	14.19
4e	7.14	16.9	10.61	17.98	10.39
Pref. occup.		16k ₁ , 16k ₂ , 8j ₂	16k ₁	16k ₁	8j ₁

- Preferential occupations of the 16k₁, 16k₂ and 8j₂ sites by Co alone
- If with La, Co occupies the 16k₁ site preferentially
- If with Ce, Co occupies the 8j₁ site preferentially



Summary

- Several promising compositions with La, Ce, Y, Co and Ni as doping elements with good HT remanence and/or enhanced performance-cost ratio are identified through BO approach, which could impact the development of novel magnet for HT application.
- La-Co pair shows the good HT remanence ($>150^{\circ}\text{C}$) over the pristine magnet and Ce-Co pair, possibly due to the specific site occupation of the elements in the lattice.



**THANK YOU FOR YOUR
ATTENTION!**

